An assessment of tidal energy potential. The Lima estuary.

A. Trigo-Teixeira[1] and I. Rebordão[2]

[1] Department of Civil Engineering and Architecture,
Instituto Superior Técnico, Lisbon Technical University,
Av. Rovisco Pais, 1049-001 Lisboa, Portugal
E-mail: trigo.teixeira@civil.ist.utl.pt

[2] WW Consulting Engineers,
Laveiras, Caxias 2760-032, Portugal,
E-mail: irebordao@wwsa.pt

Abstract

A hydrodynamic model was set up for the Lima estuary (Portugal) and a preliminary assessment of the strength of tidal currents to produce tidal energy was made. To calibrate the model results were compared with measured data, and the model tuned to reproduce water levels and currents in several locations within the estuary. The data was acquired with ADCPs, during a field campaign that was planed to cover a spring-neap tide cycle, in October 2006. The Advanced Circulation Model - ADCIRC was forced with the most important harmonic constituents present in the ocean tide signal. Upstream, in the river boundary, the discharge was taken from hydrographs. The wetting and drying tool was also applied and a detailed bathymetry was considered, since there are areas in the domain where salt marshes occur, drying out at low tide. The tidal currents potential were assessed for a scenario of tidal forcing only, without any river discharge. The lower estuary is occupied by the port infrastructure and navigation channels which conflicts with any kind of equipment installation. Values of the currents and water depths given by the model indicate that some places in the main channel of the middle estuary, might be interesting to install micro turbines in the future, depending on the evolution of the requirements of this technology.

Keywords: Tidal current energy, hydrodynamic modelling, Lima estuary, ADCIRC model, wetting and drying.

Nomenclature

x, y = cartesian co-ordinate system
u, v = velocity vector
t = time

© Proceedings of the 8th European Wave and Tidal Energy Conference, Uppsala, Sweden, 2009

1 Introduction

The urge to exploit alternative and clean energy sources is a driving force for the development of new technology. Tidal currents in some places in estuaries have a high kinetic energy associated that can be exploited. In this analysis the Advanced Circulation Model -ADCIRC was applied to describe the coastal tidal circulation induced in the Lima estuary. The study began with a preliminary analysis of similar ADCIRC applications. Then an introduction to the ADCIRC model was made. The study proceeded with the model setup that required a simplification in the bathymetry data in the shallower areas. The model calibration was made by comparison with data obtained during a measurement field campaign. This allowed the choice of the more accurate parameters to describe the circulation observed. In order to take the real bathymetry into account, without simplifications, an important feature of ADCIRC model was considered: the wetting/drying tool. The consequences of modelling the flooding and drying of the salt marshes were of importance, since the precision of the model improved considerably. Finally, the model was used to simulate the tidal propagation only, which allowed the assessment of tidal current energy, since in this scenario the forcing considered was just the ocean astronomic tide signal. This led to conclusions about the energy potential of tidal currents in the Lima estuary, after some research was made on the literature looking at the site requirements to operate these devices.

2 ADCIRC Model

The Finite Element Hydrodynamic Model created by Rick Luettich, North Carolina University and Joannes Westerink, Notre Dame University [1], was projected for coastal oceans, inlets, rivers and floodplains applications. The model is based on the solution of the generalized wave equation formulation of the governing equations on a highly flexible unstructured grid. The basic equations in a geographic coordinate system are defined as follows:

$$\frac{\partial U}{\partial t}+\frac{U}{R\cos\phi}\frac{\partial U}{\partial \lambda}+\frac{V}{R}\frac{\partial U}{\partial \phi}-fV-\frac{UVsen\phi}{R\cos\phi}= =-\frac{g}{R\cos\phi}\frac{\partial(\zeta-\alpha\eta)}{\partial\lambda}-\frac{\tau_{bx}}{\rho_0 H} \quad (1)$$

$$\frac{\partial V}{\partial t}+\frac{U}{R\cos\phi}\frac{\partial V}{\partial \lambda}+\frac{V}{R}\frac{\partial V}{\partial \phi}+fU+\frac{UVsen\phi}{R\cos\phi}= =-\frac{g}{R}\frac{\partial(\zeta-\alpha\eta)}{\partial\lambda}-\frac{\tau_{by}}{\rho_0 H} \quad (2)$$

$$\frac{\partial \zeta}{\partial t}+\frac{1}{R\cos\phi}\frac{\partial (UH)}{\partial \lambda}+\frac{1}{R\cos\phi}\frac{\partial (VH\cos\phi)}{\partial \phi}=0 \quad (3)$$

were t is time, λ and ϕ are the longitude and latitude (in degrees), ζ is the free surface elevation, U e V are the depth average-horizontal velocities, $H = \zeta + h$ is the water column depth, h is the bathymetric depth, f is the Coriolis parameter, ρ_0 is the reference density, g is the gravitational acceleration, α is the Earth elasticity factor, η is the Newtonian equilibrium tidal potential, τ_x and τy are bottom stresses in x and y directions

3 Model Setup

The ADCIRC model can work with both coordinate systems (cartesian or geographic). For the present study the geographic system was chosen. This option makes it possible to use the tidal harmonic constituents in the ADCIRC's database to define the ocean boundary condition. The bathymetric data was converted to the desired system referenced to the WGS 1984 ellipsoid and it was referenced to the local mean sea level. Due to the relative small size of some docks in the estuary area, some of those structures were left out of the model domain. The consideration of these docks would require the existence of tiny elements in order to describe them well and this would add unnecessary complexity to the mesh and constrain the time step of the model. Fig 1 shows a general view of the middle estuary.

Figure 1: General view of the Lima river. Middle estuary.

The estuary was considered well mixed and the 2D version of the model was used. The unknowns are the depth averaged velocities and the water depth. The ADCIRC model works with unstructured meshes comprising linear triangular elements. It uses the Finite Element Method to solve the differential equations describing the phenomena under consideration. The quality of the mesh is an important issue because it leads to a better model stability and to more accurate results. The mesh created for this domain was built based upon two adjacent zones. The first zone includes the ocean up to the estuary entrance. Here the mesh has an element gradation consistent with the depth, meaning that the ocean elements are bigger and the ones near the coast are smaller. It was forced for the elements to decrease in size, as they were getting closer to the estuary entrance. The second zone comprises the remaining of the estuary domain and the river, for 20 km, approximately. In this zone the mesh has small elements with a more constant size. The final mesh resulted through the merging of both meshes Fig 2. It has 10706 elements, 6039 nodes, a minimum grid spacing of 22,2 m and a maximum grid spacing of 795,5m.

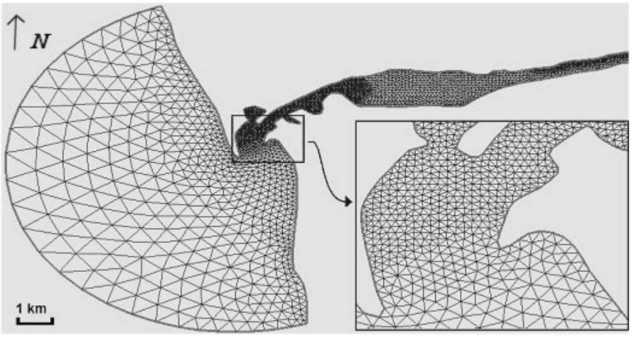

Figure 2: Finite Element Mesh and detail in the mouth of the estuary.

Three different formulations can be applied to the bottom stresses. The friction term, τ^*, can be expressed in a linear formulation (4), in a quadratic formulation where C_f is constant (5), or in a hybrid formulation where C_f is expressed by the equation (6)

$$\tau_* = C_f \quad (4)$$

$$\tau_* = \frac{C_f (U^2+V^2)^{1/2}}{H} \quad (5)$$

$$C_f = C_{f\,\min}\left[1+\left(\frac{H_{break}}{H}\right)^{\theta}\right]^{\lambda/\theta} \quad (6)$$

In the equation (6) C_f min, Hbreak (wave breaking height), θ and λ are constant terms.

In (6) C_f approaches C_f min in deep water, where H > H_{break}, and approaches C_f min $(H_{break} / H)^y$ in shallow water, where $H < H_{break}$. The exponent θ determines how rapidly C_f approaches each asymptotic limit and λ determines how rapidly the friction coefficient increases as the water depth decreases.

The quadratic bottom stress formulation, with C_f ~ 0.0025, is the recommended for the major part of the coastal simulations. On the other hand, the hybrid equation is recommended in domains with shallow waters, specially, when wetting/drying is considered. The three bottom stress formulations were experimented. The best results were obtained using the hybrid and the quadratic formulation. There was an attempt to use the recommended values of C_f in both formulations but that value led to unstable simulations. The best values obtained were C_f = 0.004 for both formulations [2].

Another issue is the time-step of the model to use. This is related to the model stability and its appropriated selection is crucial to the total computational time. It is possible to determine a maximum value to this parameter applying the Courant-Friedrich-Levy (CFL) condition:

$$Cr = \frac{\sqrt{gh}\Delta t}{\Delta x} < 1 \qquad (7)$$

where Cr is the Courant number, g is the gravitational acceleration, h is the depth in each mesh node, Δt is the time-step and Δx is a measure of the element size.

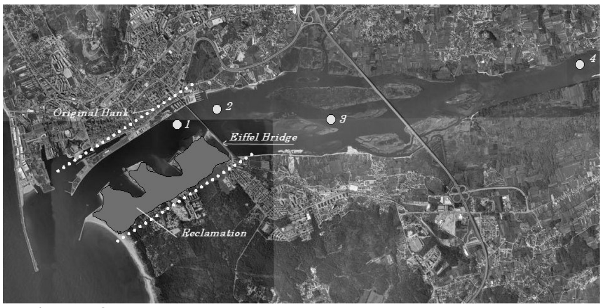

Figure 3: Lower estuary showing the location of the port infrastructure and the sites of the field campaign.

As shown, this condition is linked with the mesh and the finer the mesh resolution, the smaller the time-step must be. A time-step of 2 s was initially used [3-4].

The first runs were made with a simplified version of the bathymetry imposing a minimum water depth of 1 m in all mesh nodes. In this way the instability associated with the wetting and drying of the nodes was avoided. The calibration was made by comparing the model results with the observed data acquired through a measurement campaign conducted by the Compass Hydrographic Services Ltd [5] providing measurements at four sites, Fig 3. This campaign was carried out in October of 2006, covering a spring neap cycle. The data was adjusted in order to take into account the atmospheric pressure fluctuations. Therefore, the data values refer to the astronomic tidal only. The water surface elevation and the magnitude and direction of the velocity vectors were the variables compared. A local fisherman accidentally disrupted the instrument positioned at Site 2 and the data from this site was not used.

It was also possible to compare the water surface elevation in a site at the entrance of the estuary where Viana do Castelo's tide gauge is located.

In general, there is a good agreement between the model water levels and the data. However an increasing lack of precision in the more upstream sites was noted. The velocity results were not as good as the levels, but in general they capture the ebb-flood asymmetry well.

4 Boundary Conditions

Two main boundary conditions were considered. In the ocean boundary the water level was imposed and in the river the discharge was considered. The condition on the ocean boundary can be defined by using an ADIRC feature that imports the tidal harmonic constituents from an internal database (LeProvost database) that associates up to thirteen tidal constituents to the geographic nodes that belong to the ocean boundary. Simulations using the ADCIRC database with five tidal harmonic constituents (K_1, M_2, N_2, O_1 and S_2) and using all thirteen available constituents (M_2, S_2, N_2, MU_2, K_2, T_2, L_2, $2N_2$, K_1, O_1, P_1, Q_1 and NU_2) were tested. Another experiment was to force the model with the introduction of the tidal sinusoidal curve built with the Tidal Table values. Simulation showed that the use of all tidal constituents available in the database led to the most accurate results. The introduction of the synthesized Tidal Table curve turned out to be a slightly better option when compared with the use of only five tidal constituents.

The flow in the Lima River can also affect the study area despite the influence of a strong modulation from a dam upstream. For the simulation period, the values for the instantaneous flow were found for the closest available hydrometric station (*Ponte da Barca*). The river flow is usually very small and the highest values are due to the discharges that come from the Touvedo's dam that controls the discharge turbinated from a dam upstream. Therefore it was decided to adopt a constant value to define the river flow. The average discharge value in October is 35 m^3/s. This value was introduced in the model with an initial ramp period. The simulations with that discharge improved the results, when compared with a simulation that does not consider any river flow.

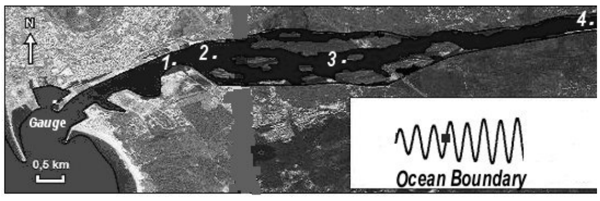

Figure 4: Model results over an aerial map. Wet and drying of the mudflats at mid tide in flow phase..

5 Wetting and drying

The tidal circulation in the estuary in a more precise way was modelled by considering the real bathymetry with the observed sand banks and mudflats within the domain. In order to do that the wetting/drying tool was applied. This function comprises an algorithm that assumes the wet and drying of the elements in the mesh.

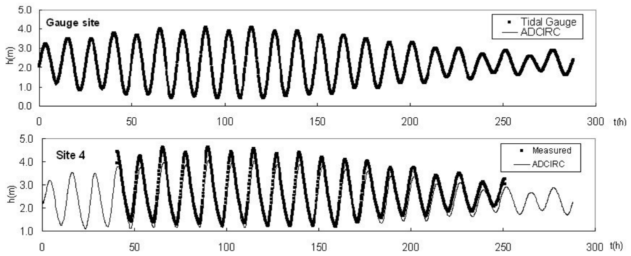

Figure 5: Surface water elevations in tidal gauge site and Site4. Comparison between ADCIRC model with the option wet/drying activated and measured values.

Each node of the mesh is defined as dry, interface or wet node. According to the node connection, each element can also be considered as dry or wet. The assessment for each node is made with reference to a minimum wetness height, *Hmin*, which can be defined by the user. The user ca also define the number of time steps that a node has to remain wet before it can be turned off and the minimum time-step in dry conditions. In addition the user can define a minimum velocity, V_{min}, which has to be checked during the wetting/drying node passage process [6-11]. In this model a value of 0,05 for H_{min} was used, a minimum value of twelve time-step for wet and for dry conditions and a V_{min} equal to 0,05 m/s.

Due to stability constraints a time-step of 0,25 s and a value of 30 for the lateral viscosity were used. These problems led also to a reduction in the mesh extension comprising now 8 322 elements and 4 649 nodes. In this simulation the best parameters chosen in the last section, with C_f = 0,0025, were used. Fig 4 shows an instant of the simulation with wet and drying .

6 Comparison with measurements

Fig 5 depicts the result of the water surface elevation and of the comparisons made for the Viana do Castelo tide gauge and for the most upstream site (Site 4). The period of the simulation is longer than the period of measurements to allow for an initial spin up of the model, which runs from a cold start. The tidal gauge site is located close to estuary entrance and at this point the tide is still the ocean tide with no deformation. The graph shows a strong sinusoidal signal of the semi-diurnal type with a fortnightly modulation of the spring-neap cycle. The tidal range in spring tides is almost 4.0 m and in neap tides is around 1.0 m. The simulated water surface elevation by ADCIRC model coincides with the synthesised curve based on the tidal tables. This is an important point, since it confirms the accuracy of the LeProvost database for the harmonic constituents in defining the ocean boundary conditions. As it happened with the results during the calibration phase the water level shows a good representation.

On the Site 4, located in the upper estuary, the deformation of the tidal curve is notorious. The simulated and the measured curves are in phase. The time of occurrence of high water is reproduced well by the model and the model captures the asymmetry between flood and ebb. The period of flood is shorter than the ebb period, and the slopes of the ascending and descending phase of the tide are also different. The model slightly under predicts the water surface elevations at this point in a consistent manner. [3].

Due to the fact that the model is 2D and represents depth averaged current velocities and the flow in reality is 3D, current velocities are more difficult to simulate than surface water levels. In Fig 6 the current velocities measured in Site1 and Site4 are compared with the currents simulated by the model. On the Site1 the model reproduces well the asymmetry between ebb and flood, the instants of slack water and the magnitude of the current in flood and the ebb periods. It can be seen that on this site the ebb dominates over flood. Results are better in the neap tide period when the amplitude of de tide is smaller. There are some spikes and noise in the measured values that the model cannot reproduce.

The measurements taken at Site 4, located in the upper estuary, show a pattern of current that does not change significantly between neap and spring tides. The graph shows that the pick magnitude of the current velocity in ebb varies between 0.4 and 0.6 m/s and that the asymmetry between ebb and flood is less well defined than in the lower estuary. The model underestimates the value of the current throughout the simulation period. In spring tide reverses the dominance between ebb and flood making the flood to prevail. However in neap tides the pattern of dominance between flood and ebb is preserved.

The acoustic Doppler current profilers were installed in the bottom measuring the three components of the current velocities on several bins in the water column at predefined sampling intervals. The vertical velocity was disregarded and an averaging process to get the mean current velocity along the water column was made, considering also the water depth at each instant. The difference between the measured and simulated current velocities can also be explained by some three dimensionality of the flow in certain locations. Despite the fact that the locations were carefully selected, far from any morphological features that could induce vortexes, recirculation or generate a vertical component of the velocity, the records always show to a greater or lesser extent a residual vertical component of the velocity field.

The model results of the direction of the current show that the model also properly describes the physics and is in accordance with what was expected in each site for a flow that is strongly influenced by the boundary geometry. The measured values reveal differences in the current direction of 180º, which correspond to a total reverse of the flow direction between the ebb and the flood. Just in Site2 small signs of current rotation are present [3].

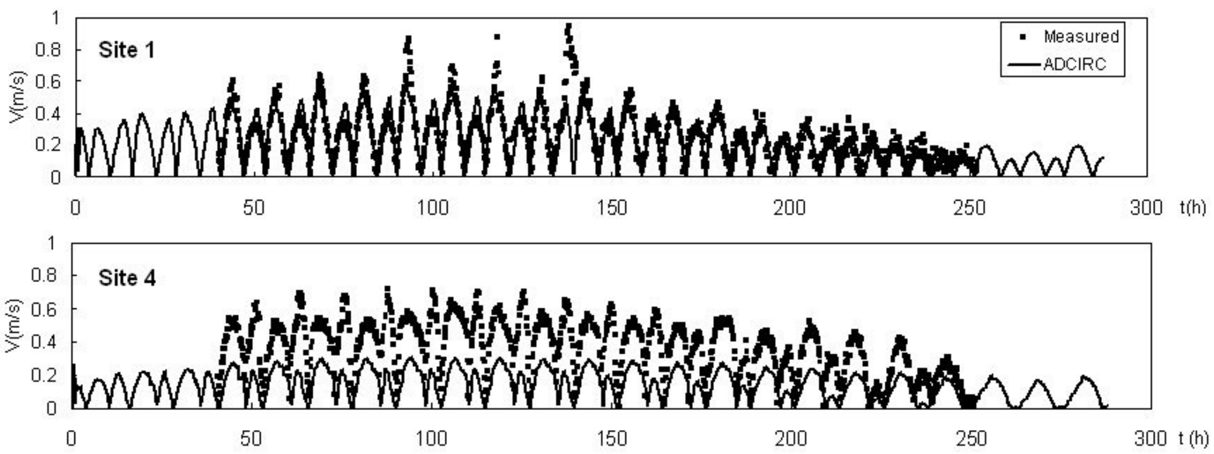

Figure 6: Currents in Site 1 and Site 4. Comparison between ADCIRC model with the option wet/drying activated and measured values.

7 Tidal energy

The most traditional tidal energy production method uses the difference in head of the tide between ebb and flood. It requires the construction of a dam and a reservoir. The water will fill the reservoir during the flood phase. When the water level starts to drop in the ebb phase a gate is closed and the water is retained creating a hydraulic head. When there is enough head, the water can flow producing energy in the turbines. Since the sixties, the largest tidal dam using this system is located in the estuary of the river Rance, in France. This method of capturing tidal energy has many disadvantages. The investment that has to be made to build the dam is high. So is the construction period. Another disadvantage in this technique is the great environmental impact on the local ecosystem. All these particularities add a non-competitiveness factor to this system [12]. A more attractive method to produce energy from tides is under development, consisting of a system that captures the kinetic energy within the constant movement of the tidal fluxes. The energy production is obtained through the use of tidal turbines installed underwater. Due to the higher water density, when compared with the air, these tidal turbines can generate the same energy as a wind turbine although requiring lower velocities and smaller areas of the blades. The tidal systems are more predictable than the wind, since they are not affected by the meteorology Tidal turbines present several advantages: an easy installation; minor visual impact; they don't cause significant impact to the sea life and navigation can pass over or be diverted in some cases. On the other hand, the turbines face some problems that are still under investigation, like the strong drag forces; the development of plants on top of the blades; corrosion; damages from storms and in some places they can obstruct navigation. Many different tidal turbines systems are under development. For example, they can differ in features like rotation axis (vertical or horizontal), the rotor (with or without a duct) or the type and number of blades. The mooring systems can be gravity base, mono-pile, piled-jacket and floating.

The first two are recommended for shallow waters. In general, systems can be found that require velocities between the 0,5 m/s and 6 m/s. The devices also require a minimum water depth for installation. However, micro turbines can operate in very shallow water.

8 Energy assessment in the Lima Estuary

To characterize the potential to generate energy from tidal currents some basic laws must be presented. The power in a section of the estuary depends on the current velocity and on the area of the section and can be calculated by:

$$P = \frac{1}{2}\rho \int_A V^3 dA \qquad (8)$$

Equation (8) gives an estimate of the potential of tidal fluxes in the estuary in a certain location. The power of the turbine *Pt* is dependent on the efficiency of the device and on the area of the turbine projected in the direction of the flow field:

$$P_t = \frac{1}{2}\eta\rho A U^3 \qquad (9)$$

where: η is the turbine efficiency, ρ the water density, A the area of the turbine in the direction of the flow and U the mean velocity of the flow. Hence, the potential depends mainly on the strength of the tidal currents. Here, it is assumed that the mean velocity of the current can characterize this strength.

Equation (9) shows that the sites with higher current velocities are the most favourable for the installation of a tidal system. However, the local bathymetry is also a factor to consider. The bathymetry of the Lima estuary referred to the mean sea level is shown in Fig 7.

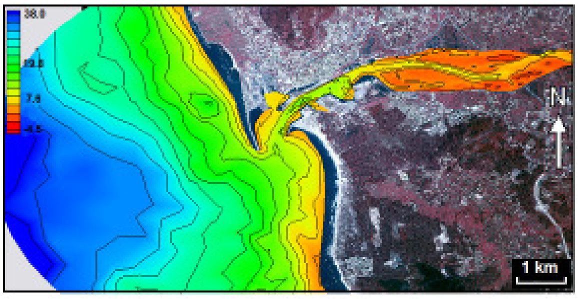

Figure 7: Bathymery referred to mean sea level.

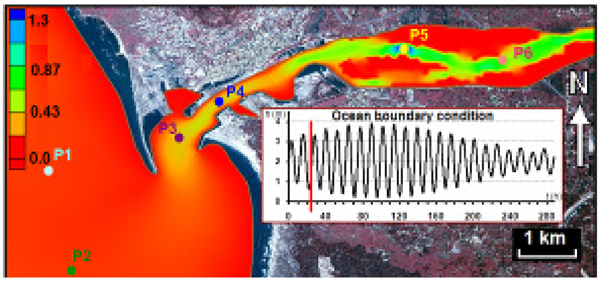

Figure 8: Velocity field in a flow phase.

The results of the simulation in the spring-neap cycle showed velocities ranging from 0 and 1,34 m/s. Six sites to evaluate the potential were chosen. These sites are shown in Fig 8. In this picture the flow filed in a flood phase is also presented. The values of the current velocity for the points selected are presented in Table 1

		Current velocity [m/s]		
Site	Depth [m]	Average	Max	Min
P1	20,3	0,037	0,090	0,001
P2	25,2	0,037	0,085	0,001
P3	7,2	0,147	0,425	0,002
P4	12,2	0,154	0,412	0,000
P5	4,5	0,380	1,297	0,000
P6	3,9	0,227	0,573	0,000

Table 1: Current velocity in five sites in the Lima Estuary.

It was observed that the sites P1 and P2 being outside the estuary in open waters have insignificant velocities; therefore the option of installing any tidal equipment there is impossible. Sites P3 and P4 have very low current velocity and since those sites are located in the port area they conflict with navigation. The installation of the tidal energy structures is not possible without interfering with the navigational channel. Sites P5 and P6 have the highest velocities, however the depth does not seem to be sufficient for the installation of tidal energy systems. However, in site P5, in the main channel of the middle estuary, the situation can be studied further in the future for the installation of a tidal system that associate elements forming a fence across the channel in order to use part of all the section flux available in that site.

9 Conclusions

The demand of renewal energy is the driving force for the assessment of the energy potential of tidal currents. The idea to produce energy directly from the currents is very attractive since the deployment of devices into the water does not require any kind of damming. The environmental impacts are lower and turbines and associate devices can be mass-produced and improved. The amount of energy can be estimated accurately since is not directly influenced by the meteorology of the site selected.

Mathematical models play an important role in resolving the flow in coastal waters and estuaries where tidal fluxes are expected to occur. In this study the ADCIRC model was used to study the tidal propagation in the Lima estuary in the north of Portugal. A detailed model of the estuary was set-up and calibrated. For the calibration of the model, a measurement campaign was conducted acquiring data in four sites four currents and surface water levels. The model results show the importance of the wetting/drying tool, especially to describe the water circulation in the shallow zone of the estuary were salt marshes occur.

Six locations were analysed regarding the potential for the installations of tidal turbines. In general, outside the port area, low current velocities and a shallow bathymetry characterize the estuary. However, a location was identified in the main channel of the middle estuary with some potential. With the development the tidal energy equipment of the fence type and micro-turbines, it may be possible to look at this site, with new and favourable perspectives relating the tidal energy production.

Acknowledgements

The authors would like to thank the Division of Design Support Systems of the Department of Civil Engineering and Architecture of Instituto Superior Técnico for the conversation of the bathymetry scatter sets from cartesian into geographic coordinates and all support given. The financial support of CEHIDRO – Centro de Estudos de Hidrosistemas of Instituto Superior Técnico is also acknowledge.

References

[1] J.J. Westerink and R.A. Luettich. Tide and Storm Surge Predictions in the Gulf of Mexico using model ADCIRC-2D. *Report to the US Army Engineer Waterways Experimentation Station*. 1991.

[2] I. Rebordão. Análise do Potencial Energético dos Fluxos de Maré no Estuário do Lima. Lisbon, Portugal: Instituto Superior Técnico, Master Thesis, 78p. 2008.

[3] I. Rebordão and A. Trigo-Teixeira. Tidal Propagation in Lima Estuary. *Journal of Coastal Research, SI 56*, Lisbon, Portugal. 2009.

[4] A. Trigo-Teixeira. Dredging Works in Port of Viana do Castelo and the Impact on the Eiffel Bridge. A Case

Study Using Finite Element Hydrodynamic Modeling. *PIANC Med Days*, Palermo. 2008.

[5] Hidrodata Staff. Relatório Levantamento Topo-Batimétrico, Campanha de Medição de Correntes e Níveis e Recolha de Amostras 0506-A2P. Lisbon. Portugal. 2006.

[6] M. Aggarwa. Storm Surge Analysis Using Numerical and Statistical Techniques and Comparison with NWS Model Slosh. *Office of Graduate Studies of Texas A&M University. Texas.* Master's thesis. 2004.

[7] J.C. Dietrich, R.L. Kolar, and R.A. Luettich. Assessment of ADCIRC's Wetting and Drying Algorithm - *School of Civil Engineering and Environmental Science*, University of Oklahoma, Norman, 73019. 2004.

[8] O. Gourgue, E., Deleersnijder and V. Legat. A Finite Element Wetting-Drying Method, with Application to the Sheldt Estuary, *Geophysical Research Abstracts*, vol. 10, EGU2008-A-00712. 2008.

[9] D. Dietsche, S.C. Hagen, and P. Bacopoulos. Storm Surge Simulations for Hurricane Hugo (1989): On the Significance of Inundation Areas. *Journal of Waterway, port, Coastal and Ocean Engineering,* Vol. 133, No. 3. 2007.

[10] Ş, N. Ertürk, N. A. Bilgili, M. R. Swift, W. S. Brown, B. Çelikkol, J.T.C. Ip and D.R. Lynch, Simulation of the Great Bay Estuarine System: Tides with Tidal Flats Wetting and Drying, *J. Geophys. Res.,* 107(C5),3038, doi: 10.1029/2001JC000883. 2002.

[11] Z.-G. Ji, M. R. Morton, and J. M. Hamrick. Wetting and Drying Simulation of Estuarine Processes. *Estuarine, Coastal and Shelf Science,* 53, 683-700. doi: 10.1006/ecss.2001.0818. 2001.

[12] J. Andrews and N. Jelley. Energy Science Principles, Technologies and Impacts. Oxford University Press. 2007.